AMERICAN JOURNAL of PHYSICS

Unveiling the physics of the Thomson jumping ring

Celso L. Ladera and Guillermo Donoso

Citation: American Journal of Physics **83**, 341 (2015); doi: 10.1119/1.4902891
View online: http://dx.doi.org/10.1119/1.4902891
View Table of Contents: http://scitation.aip.org/content/aapt/journal/ajp/83/4?ver=pdfcov
Published by the American Association of Physics Teachers

Unveiling the physics of the Thomson jumping ring

Celso L. Ladera[a)] and Guillermo Donoso
Departamento de Física, Universidad Simón Bolívar, Caracas 1086, Venezuela

(Received 6 January 2014; accepted 14 November 2014)

We present a new theoretical model and validating experiments that unveil the rich physics behind the flight of the conductive ring in the Thomson experiment—physics that is hard to see because of the rapid motion. The electrodynamics of the flying ring exhibits interesting features, e.g., varying mutual inductance between the ring and the electromagnet. The dependences of the ring electrodynamics upon time and position as the ring travels upward are conveniently separated and determined to obtain a comprehensive view of the ring motion. We introduce a low-cost jumping ring setup that incorporates pickup coils connected in opposition, allowing us to scrutinize the ring electrodynamics and confirm our theoretical model with good accuracy. This work is within the reach of senior students of science or engineering, and it can be implemented either as a teaching laboratory experiment or as an open-ended project.
[http://dx.doi.org/10.1119/1.4902891]

I. INTRODUCTION

Many published works on the Thomson jumping ring experiment naturally focus on how high the electromagnet is capable of throwing the conductive ring. A dramatic launch was indeed the original purpose of Thomson in the 1880s, during the debate between dc and ac for public power distribution networks, when it was crucially important to show that ac currents could do work. The sight of the ring suddenly flying upward still delights audiences today. But the thrust happens so quickly that little attention is paid to the rich physics behind the experiment. We frequently hear that "it can all be explained by applying Faraday's law and Lenz's law." In some instances, the circuit of the thrusting device incorporates a large charged capacitor, which, when rapidly discharged through the electromagnet, propels the ring several meters high.

Nonetheless, the last two decades have seen interesting works published on the subject, in which more details of the physics behind Thomson's experiment have been clarified.[1–6] For instance, the seldom-demonstrated levitation of the ring on the electromagnet, the time the ring takes to depart from the near vicinity of the electromagnet, and the dependence of the force upon the frequency of the alternating current are now receiving attention. We recently published a paper[5] in which the explicit functional dependences of the ring motion on the most relevant variables were theoretically and experimentally found and demonstrated. For instance, we showed how to measure the instantaneous current induced by the electromagnet in the ring itself, and we measured the magnetic force on the ring as a function of the excitation current for increasing current frequencies.

In this work, we focus on the flight of the ring, to unveil both theoretically and experimentally, in a detailed way, how that flight depends on a number of parameters. The variables that we examine include the number of cycles of the applied ac excitation to the electromagnet, the current in the electromagnet coil and its relation to the mutual inductance between ring and electromagnet, the ring velocity and acceleration functions, the force on the ring as a function of height, and even the height dependence of the actual emf induced in the ring. Our experiments are performed using a modest-size jumping ring apparatus and our ring reaches only several tens of centimeters high, with modest coil currents, but our results and conclusions are valid for the more massive versions of the experiment.

Our apparatus incorporates new sensors to scrutinize the ring motion and its physics, and thus we obtain experimental results that to our knowledge have not been published before. Two long vertical pickup coils wound over the electromagnet allow us to measure variables such as the actual current induced in the ring and the varying mutual inductance of the transformer-like system. An LED-illuminated slit source plus a phototransistor device allows us to monitor the ring position accurately along its vertical flight. We also present a new analytical approach in which the dependences of the ring electrodynamics upon time and position are conveniently separated and determined, and then validated by the experiments presented in Sec. IV. Both our theoretical model and our experiments—performed with a minimum of instrumentation—are within the reach of undergraduate students in science or engineering. This work is appropriate for implementation as a low-cost senior physics laboratory experiment or an open-ended student project.

II. A DETAILED ANALYTICAL MODEL

Consider the jumping ring setup illustrated in Fig. 1. The conductive ring is coaxial with an electromagnet, whose coil (called the *main coil* below) is excited with an ac current of known angular frequency ω. We determine the entire motion of the ring along the vertical z-axis by solving its equation of motion. This is not a straightforward task because the ring moves through a time-varying non-uniform magnetic field created by an electromagnet whose electrical parameters depend on the motion of the ring itself.

The instantaneous magnetic force on the ring is given by the standard textbook expression[1–6,8,9] for the force exerted by a magnetic field on a ring current

$$F(t) = i_{\mathrm{ring}}(t)\,2\pi a\,B_\rho(t), \tag{1}$$

where a is the mean radius of the ring and i_{ring} is the (time-varying) current induced in the ring by the (time-varying) magnetic field of the electromagnet. Here, $B_\rho(t)$ represents the harmonically varying radial component (of amplitude $B_{\rho,m}$) of that field

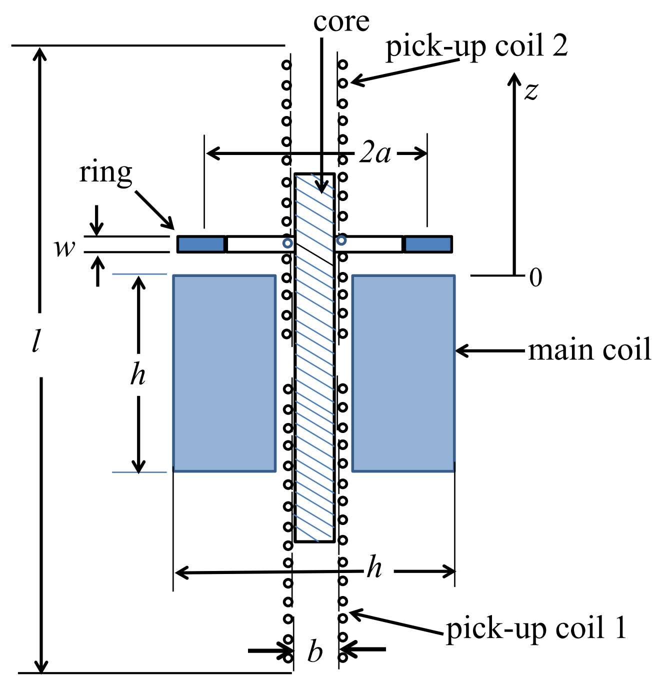

Fig. 1. Longitudinal section of our jumping ring setup showing the long core (30 cm long, square cross section of side $b = 4$ cm), the main coil ($h = 6.5$ cm) of the electromagnet, and the ring at the top (mean radius $a = 3.65$ cm, $w = 10.0$ mm). Two long pickup coils 1 and 2, connected in opposition, are wound around the core. Each pickup coil has 2 turns/cm and is 19 cm long, so $l = 38$ cm.

$$B_\rho(t) = B_{\rho,m} \sin \omega t, \tag{2}$$

for an exciting current $I_c(t) = I_m \sin \omega t$ in the main coil. The instantaneous current in the ring is given by the quotient of the emf $\varepsilon_i(t)$ and its electrical impedance $Z(z)$. Here, $\varepsilon_i(t)$ can be obtained by applying Faraday's law to the time-varying axial magnetic flux of the core (assumed to have squared cross section of area b^2), i.e., to the flux of the vertical component $B_z(t)$ of the main coil field[7]

$$\varepsilon_i(t) = -\frac{d}{dt}\left[b^2 B_z(t)\right] = -\omega\, b^2 B_{z,m} \cos \omega t. \tag{3}$$

Meanwhile, the electrical impedance $Z(z)$ is not constant but is a function of the ring's vertical position z as the latter flies upward, and is given by $Z = \sqrt{R^2 + \omega^2 L(z)^2}$, where R and $L(z)$ denote the resistance and inductance of the moving ring, respectively. As seen in Fig. 1, we fix the origin $z = 0$ of the vertical coordinate axis at the top of the electromagnet (where the ring rests when no electrical current is applied to the electromagnet). The varying inductance of the ring as the ring moves upward shall be later conveniently written as $L(z) = l(z)L_0$, where L_0 is the nominal self-inductance of the ring (a purely geometry-dependent parameter) and $l(z)$ is a functional factor that accounts for the vertical position dependence of the ring inductance. It is important to recognize that as the ring travels upward, it does so across the non-uniform magnetic field region above the electromagnet, where the magnetic field lines are divergent and their density diminishes as the ring's vertical position increases (the field weakens both radially and axially). Therefore, all of the relevant electrodynamics variables of the ring vary with its vertical position and time.

It is convenient to separate the functional dependences of the axial component of the magnetic field on time t and vertical coordinate z as follows:

$$B_z(t) = B_{1z}\, b_z(z)\, I_c(z,t), \tag{4}$$

or

$$B_z(t) = B_{1z}\, b_z(z)\, I_c(t) I(z), \tag{5}$$

where B_{1z} is the constant value of the axial field component at the top of the electromagnet core (at $z = 0$) per unit of current in the coil. Here, $b_z(z)$ is an auxiliary factor that represents the axial variation of the magnetic field produced by the magnetic permeability of the electromagnet core. This $b_z(z)$ can be readily determined experimentally and is defined so that $b_z(0) = 1$. Moreover, $I(z)$ is the auxiliary functional factor that incorporates into our model the decrease produced in the coil-exciting current by the vertically varying mutual inductance between the ring and the coil. It is also an auxiliary function to be determined as will be explained below (Appendix A). The two components of the electromagnet's field can also be obtained theoretically with some extra effort (because of the electromagnet core), using the treatment of coil fields presented in Ref. 10.

In analogy to Eq. (4), the radial component of the magnetic field can be written as

$$B_\rho(t) = B_{1\rho}\, b_\rho(z)\, I_c(t) I(z), \tag{6}$$

for the coil current $I_c(t) = I_m \sin \omega t$. We can then rewrite the two field components as

$$B_z(z,t) = B_{1z}\, b_z(z)\, I(z)\, I_m \sin \omega t, \tag{7}$$

$$B_\rho(z,t) = B_{1\rho}\, b_\rho(z)\, I(z)\, I_m \sin \omega t, \tag{8}$$

where $I_c(z,t) = I(z) I_c(t) = I(z) I_m \sin\omega t$. The required emf induced in the ring can thus be written as

$$\varepsilon_i(z,t) = \omega\, b^2 B_{1z}\, b_z(z)\, I_c(0) I(z) \cos \omega t = \varepsilon_{i,\max} \cos \omega t, \tag{9}$$

so that the current in the traveling ring becomes

$$\begin{aligned} i_{\text{ring}}(z,t) &= \frac{\varepsilon_{i,\max}}{Z} \cos[\omega t - \phi(z)] \\ &= \frac{\varepsilon_{i,\max}}{\omega L}\, \sin \phi(z) \cos[\omega t - \phi(z)]. \end{aligned} \tag{10}$$

Here, $\phi(z)$ is the expected position-dependent phase difference between the ring current and the emf induced in the ring by the driving magnetic field of the electromagnet, given by $\tan \phi(z) = \omega L(z)/R$. We can then write the instantaneous magnetic force $F(z,t)$ on the ring, Eq. (1), in the convenient form

$$\begin{aligned} F(z,t) = &\frac{1}{L(z)} (2\pi a)\, b^2 B_{1z}\, b_z(z) B_{1\rho}\, b_\rho(z) \sin \phi(z) \\ &\times \cos[\omega t - \phi(z)] I_c(0)^2 I(z)^2 \sin \omega t. \end{aligned} \tag{11}$$

Note that the force at any given location oscillates at twice the frequency of the ac voltage applied to the electromagnet.

Equation (11) allows one to determine the ring electrodynamics at any height and time. Note, for instance, the appearance of the vertically varying inductance $L(z)$, which controls the coupling between the ring and the magnetic field gradient. Another quantity of interest is the *time averaged* force $F(z)$ on the magnet, which is also a function of the ring's vertical position z. We can readily obtain this average force from Eq. (11), and express it in a way that separates the influences of the axial and radial magnetic field components

$$F(z) = \frac{1}{l(z)L_0}(\pi ab^2)B_{1z}b_z(z)B_{1\rho}b_\rho(z)I_c(0)^2 I(z)^2 \sin^2\phi(z). \tag{12}$$

This average force is plotted in Fig. 2 as a function of the ring position z.

To calculate either the instantaneous force $F(z,t)$ or its time average $F(z)$, we must determine the three position-dependent auxiliary functions introduced above: $b_\rho(z)$ for the radial field component, $b_z(z)$ for the axial field component, and $l(z)$ for the varying inductance. We can find these functions with little effort, as described in Sec. V below.

Having found an expression for the magnetic force on the flying ring (of known mass m), we can now consider solving its equation of motion

$$m\frac{d^2}{dt^2}z(t) = F[z(t)] - mg. \tag{13}$$

After substituting Eq. (12) for the force $F(z)$, this equation can be solved using a numerical procedure, e.g., the second-order Runge-Kutta method or the routines used by various commercial software packages, with the initial conditions $z(0) = 0$ and $z'(0) = 0$. Note that for simplicity we have used the average force from Eq. (12), rather than the rapidly oscillating expression given in Eq. (11). The numerical solutions are essentially unaffected by the averaging, because the inertia of the ring prevents it from responding to the rapid oscillations of the force. A couple of typical solutions for the ring position $z(t)$ and its speed $z'(t)$ are plotted in Sec. IV, where they are compared with the measured position and speed of the ring.

III. APPARATUS AND EXPERIMENTAL SETUP

Our experimental setup is similar to the standard classroom apparatus: a vertically aligned electromagnet and a coaxial metallic ring, plus an ac voltage source. Our electromagnet has a 30-cm long steel core with a square cross section of width $b = 4$ cm; its 6.5-cm-long coil has 500 turns of thick copper wire (AWG 18, 1-mm diameter), and its nominal resistance and inductance are 2.5 Ω and 11 mH, respectively. The electromagnet is driven using a Variac at the 60-Hz grid frequency. In our experiments, this coil carries currents with amplitudes $I_c(0)$ in the range of 1–10 A. Our typical ring is made of aluminum stock, has a mean radius $a = 3.65$ cm, a square cross section of 10 mm × 10 mm, and a mass of 68.3 g. The initial position ($z = 0$) of our ring is at the top of the coil (Fig. 1). The resistance of the ring is a mere 0.070 mΩ, and its nominal inductance L_0 is rather small, $L_0 = 0.110\,\mu$H. A dual-trace digital oscilloscope is used to monitor the signals in the electromagnet coil and in the pickup coils shown in Fig. 1. Our magnetometer is a commercial *xyz* magnetic field Hall probe.[11]

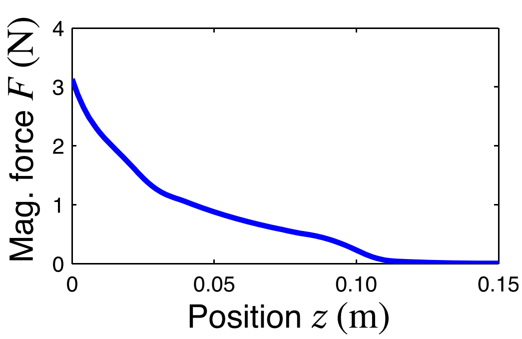

Fig. 2. Predicted magnetic force on the ring as a function of the ring position, as described by Eq. (12). The force decreases monotonically and reaches zero at about 12 cm, in coincidence with the upper end of the protruding core shown in Fig. 1.

We have incorporated additional devices into our setup in order to obtain detailed measurements of the ring electrodynamics. Along the entire electromagnet core there are two thin wire (AWG 38, 0.1007-mm diameter) elongated pickup coils, each 19 cm long, and hand-wound at two turns per centimeter on a rolled sheet of bond paper. These coils surround the vertical core (they fit into the small space left between main coil and core). These two pickup coils are symmetrically located and connected in opposition at the middle so that their signals are π radians out of phase. The upper pickup coil spans from the mid-plane of the core to about 4 cm above the top of the core, and covers the region where the ring interacts with the electromagnet's field and generates its own magnetic field. The lower pickup coil spans from the middle of the core to 4 cm below the bottom of the core, far from where the ring moves, and therefore its interaction with the magnetic field produced by the ring itself is practically nil. Because they are connected in opposition, the two pickup coils cancel the magnetic field effects of the main coil (i.e., the net signal from the two coils is only 1/250th of the signal that one unbalanced coil would give due to the ac field of the main coil) and allow us to measure the magnetic field produced by the induced current in the ring in the presence of the main coil field.

To monitor the vertical position of the ring accurately as it travels upward, we attached to it a long strip of thin transparent acrylic sheet, with a scale of 2 mm divisions along the first centimeter, and every 5 mm afterwards, ruled on it. This light strip hangs down from one side of the ring. A horizontal thin collimated beam of light, generated using a narrow slit illuminated from behind with a white LED, traverses the acrylic strip to fall on a photo-transistor followed by a diode connected to the photo-transistor emitter. As the ring moves upward we can register its position by monitoring the signal from this simple circuit with a digital oscilloscope. This position-monitoring system works very well: it gives us the ring vertical position with a resolution of about 0.5 mm (see also Fig. 5 below).

We have also resorted to an auxiliary small pickup coil, 10 turns of thin wire (38 AWG), 36.5-mm mean radius and only 1 mm high, to measure the vertical component of the electromagnet's field along the vertical axis, by simply sliding it up in small steps and measuring the magnetic flux through it.

IV. EXPERIMENTS AND RESULTS

A. Exciting current in the coil and emf induced in the pickup coils by the ring

Figure 3 shows oscilloscope traces of the exciting current in the main coil of the electromagnet (upper trace) and of the

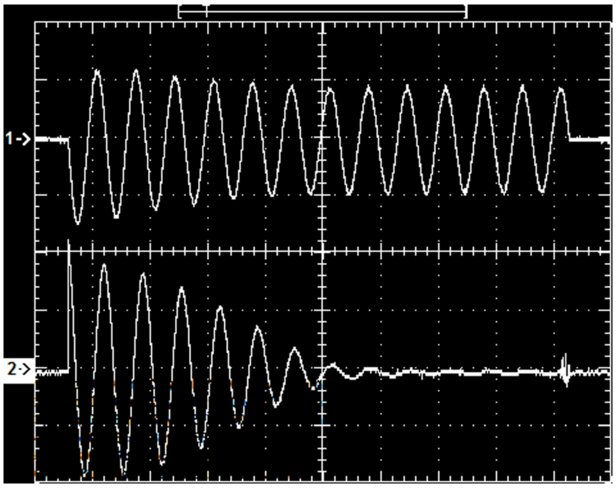

Fig. 3. Oscilloscope traces of the electric current in the main coil (top) and the emf induced in the pickup coils by the magnetic field produced by the jumping ring (bottom), for 13 cycles of 60-Hz voltage (80-V amplitude) applied to the electromagnet.

emf induced in the long pickup coils by the magnetic field generated by the ring itself (lower trace). The main coil trace corresponds to 13 cycles of 80 V constant-amplitude voltage applied to the coil with the Variac. (This voltage signal corresponds to an excitation current of amplitude about 5 A.)

These two traces contain useful information. For instance, note that in spite of the constant voltage applied to the coil, the amplitude I_m of the harmonically varying current in the coil decreases with time. We attribute this decay to the ring as it moves upward. In effect, we can think of the whole apparatus as a transformer in which the main coil is the primary while the ring plays the role of the secondary. The effective inductance L' of the coil depends on the mutual inductance M between the ring and the coil (see Appendix A). This coupling inductance M diminishes as the ring moves upward, away from the electromagnet, which means that L' increases, and so the coil impedance increases as well. Thus the coil current must diminish as the ring flies upward from the coil. The pickup coils signal (lower trace of Fig. 3) is closely related to the electrical current that appears in the ring, as we explain in Sec. IV B.

Figure 3 also shows a phase difference ϕ between the two traces, which can be directly measured by simply superposing them on the digital oscilloscope screen and marking with the two oscilloscope cursors. This phase difference arises between the induced emf in the ring and the exciting current in the main coil. The squared sine of this phase is the factor that appears in Eqs. (11) and (12), which give the instantaneous force $F(z,t)$ on the ring and the average force $F(z)$, respectively. This phase difference has been already mentioned and discussed in previous works on the jumping ring.[2,3,5]

B. Comparing the electric current in the jumping ring with the exciting current in the coil

In Fig. 4, we plot the exciting current i_{coil} in the main coil (dashed curve) and the actual induced current i_{ring} that appears in the ring (continuous curve), both as functions of time. To obtain the current in the ring we numerically integrated the induced emf that appears in the pickup coils (generated by the magnetic field of the ring, and shown in the lower trace of Fig. 3), as discussed in Appendix B. With its small nominal resistance (0.070 mΩ), the jumping ring is

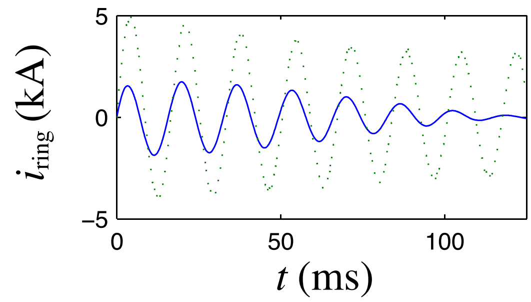

Fig. 4. Electric current in the main coil i_{coil} (A) (dashed curve) compared with the current induced in the ring i_{ring} (solid curve), plotted as functions of time. Note that the scale for i_{ring} is in kA.

seen to carry currents that can reach a thousand amperes—while the current in the main coil remains less than 10 A.

Alternatively, we also measured the integral of the emf induced in the ring (lower trace of Fig. 3) by connecting a passive RC integrator to the two pickup coil terminals. It is well known[12,13] that (provided $\omega RC \gg 1$) the output voltage of this kind of electronic integrator is proportional to $i_{ring}(t)$. We used a resistor of $R = 20\,\mathrm{k}\Omega$ and a capacitor of $C = 1\,\mu\mathrm{F}$.

C. Vertical position of the ring as a function of time

Figure 5 shows the measured ring position as it travels upward, as determined from the signal generated in the LED-phototransistor circuit that we use to detect the varying intensity of the transmitted beam of light (described in Sec. III above). In Fig. 6 we have plotted the measured vertical position of the ring as a function of time, compared to the prediction of our theoretical model (Sec. II); one data set is for an exciting ac voltage (80-V amplitude) applied for 13 cycles, while the other data set shows what happens when the exciting voltage is turned off after just 3 cycles.

As Fig. 6 shows, a thrust lasting only 3 cycles (50 ms) causes our ring to rise rapidly to a maximum height of about 10 cm in about 170 ms. When the thrust continues for 13 cycles, the ring rises about 17 cm in 200 ms. Note the close agreement between our experimental data and the predictions of our analytical model.

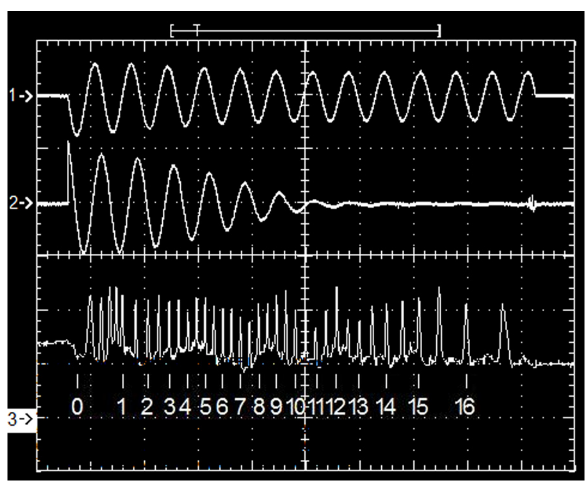

Fig. 5. Oscilloscope trace showing (in the bottom trace) the LED-phototransistor signal that indicates the vertical position of the ring as it travels upward. The superimposed cm scale indicates the actual ring position during its flight, determined by counting peaks in the signal. The traces of Fig. 3 are shown above, with the same time scale, for comparison.

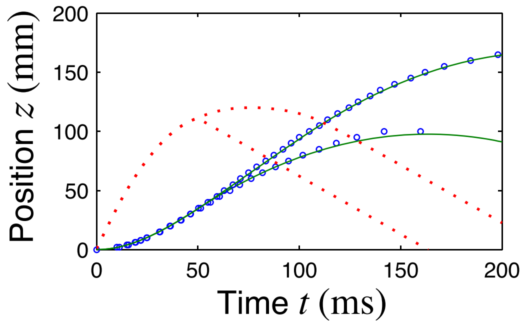

Fig. 6. Position of the flying ring as a function of time, for 3 cycles (lower continuous curve) and 13 cycles (upper continuous curve) of the applied sinusoidal voltage (80-V amplitude) to the main coil, as predicted by our theory. The dots show the corresponding experimental data. The two dashed curves show the speed of the ring (in cm/s), obtained by taking the derivatives of the continuous curves.

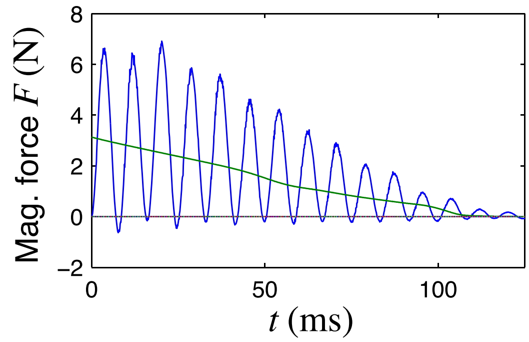

Fig. 8. Magnetic force on the jumping ring as a function of time. The oscillating curve (at twice the frequency of the applied ac voltage) represents the instantaneous force on the ring while the decaying curve represents the average force.

The dashed curves in Fig. 6 show the vertical speed $v(t)$ of the ring for both the 3- and 13-cycle thrusts. The speeds coincide for the duration (50 ms) of the first three cycles. Subsequently, in the 3-cycle case the velocity abruptly begins to decrease at a rate equal to the gravitational acceleration, while in the 13-cycle case the velocity reaches a maximum after a total of about 75 ms and then smoothly decreases as the gravitational force begins to dominate.

D. Maximum height reached by the ring

A common goal of the jumping ring experiment is to achieve the greatest possible maximum height $h_{\max}$. In Fig. 7, we have plotted our experimental values of $h_{\max}$ for three different values of the voltage applied to the main coil.

The three continuous curves in Fig. 7 were plotted using our theoretical model (Sec. II), and agree well with the experimental data. For any given voltage amplitude, the maximum height increases almost linearly with the number of cycles of applied voltage, until it reaches a plateau (e.g., after about 4 cycles for the three curves plotted in the figure). The reason for the plateau is simply that by this time the ring has left the region where the magnetic field exists, which occurs about 4 cm above the core in our setup.

E. Magnetic force on the ring as a function of time

Figure 8 compares the oscillating instantaneous magnetic force on the ring, computed from Eq. (11), to the average force, computed from Eq. (12). The instantaneous force is almost always positive (upward), but becomes slightly negative for brief intervals during each oscillation. This behavior is related to the phase difference $\phi(z)$ between the two currents: the duration of each interval of downward force is $[\pi/2 - \phi(z)]/\omega$.

The instantaneous force on the ring is proportional to the current in the ring times the excitation current in the coil and can therefore be simply obtained by multiplying the experimental values of these two currents; these measured currents are plotted in Fig. 4.

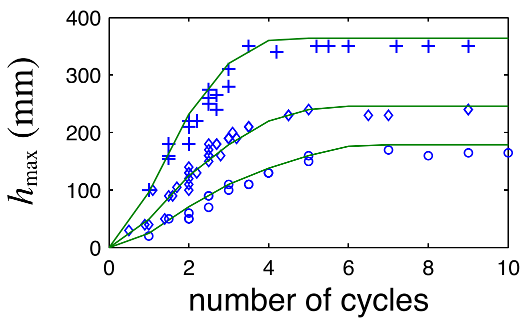

Fig. 7. Maximum height reached by the ring as a function of the number of cycles of applied sinusoidal voltage to the main coil, for voltage amplitudes of 118 V (crosses), 100 V (diamonds), and 80 V (circles). The continuous curves are the predictions of our theoretical model.

V. THE AUXILIARY FUNCTIONS

A. The axial and radial functions $b_z(z)$, $b_\rho(z)$ of the electromagnet field

In Fig. 9, we have plotted both the measured auxiliary radial function $b_\rho(z)$ at the ring (circles) and the auxiliary axial component function $b_z(z)$ (crosses) of the electromagnet magnetic field, as functions of the vertical coordinate z. The measurements of $b_\rho(z)$ were made using the xyz magnetometer, and those of $b_z(z)$ were made using the small auxiliary (1-mm long) pickup coil (mentioned at the end of Sec. III), which we slide coaxially up along the core and also above it. Note that the auxiliary function $b_z(z)$ decays almost linearly, while $b_\rho(z)$ decays abruptly above $z = 11$ cm, in coincidence with the protruding length of core (above the main coil).

B. The auxiliary function $l(z)$ of the ring inductance and the phase difference between the coil and ring currents

As was mentioned in Sec. II, the inductance $L(z)$ of the ring does not remain constant as the ring travels upward. Therefore, this inductance was written in Eq. (12) as the

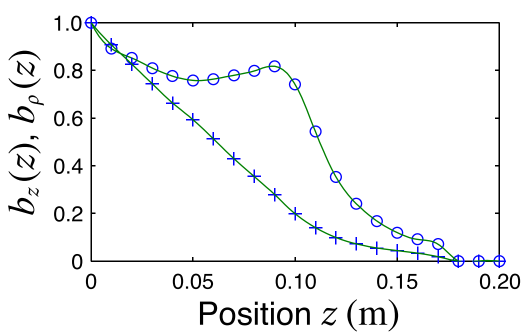

Fig. 9. Experimentally measured auxiliary functions $b_z(z)$ (crosses) and $b_\rho(z)$ (circles). The continuous lines are cubic-spline interpolation fits to the data.

product $L(z) = l(z)L_0$. Figure 10 shows the measured auxiliary function $l(z)$, a dependence that arises from the relative magnetic permeability of the electromagnet core. The other functional dependence $I(z)$ (see Appendix A) arises from the varying mutual inductance of the ring and coil.

It can be seen that this function decays from its initial value of about 3 (ring resting on top of the coil) to 1 at about $z = 11$ cm above the coil, and from there onwards it remains constant. The lower curve in Fig. 10 shows instead the squared sine of the phase difference ϕ between the induced emf in the ring and its induced electrical current. The two curves in Fig. 10 are not independent from each other, being related through $\omega L_0\, l(z) = R\tan[\phi(z)]$. The phase difference ϕ was measured in a preliminary experiment in which the ring was positioned at fixed z values and at each z we registered both the sinusoidally varying current in the coil and the sinusoidally varying emf induced in the pickup coils in the digital dual-trace oscilloscope.[5] The comparison of the two traces in Fig. 3 also provides a measurement of this important phase difference ϕ.

VI. DISCUSSION AND CONCLUSIONS

Unveiling the physics behind the flight of the Thomson jumping ring is not a straightforward task because the electromagnetic variables of the ring-electromagnet system implicitly depend on the ring motion itself. This motion takes place in a nonuniform magnetic field, and thus we face a true electrodynamics problem. In the present work, we have extended earlier investigations in several ways: First, in our theoretical model we separated the time and the position dependences of the main variables, introducing auxiliary functions that simplified our mathematical treatment. Second, a pair of long pickup coils connected in opposition, and wound over the electromagnet core, allowed us to measure the magnetic field created by the moving magnet. Third, the LED-illuminated slit-phototransistor sensing system described in Sec. III allowed us to measure the ring position with sub-millimeter accuracy.

Our experimental results include a plot (Fig. 8) of the measured instantaneous force on the ring, compared with the theoretical average force—a comparison not found in the published literature. We have shown how the mutual inductance varies with the ring height and its concomitant effect on the main coil excitation current. The dependence of the maximum height reached by the ring upon the number of excitation cycles is also presented (Fig. 7) for the first time.

As mentioned in the Introduction, the Thomson ring experiment is often intended just to show that the ring can

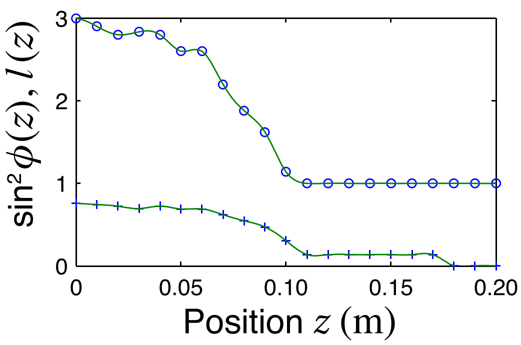

Fig. 10. Measured auxiliary function $l(z)$ (upper data set) and the function $\sin^2(\phi)$ (lower data set). The continuous curves were obtained using a cubic-spline fit to the data.

jump several meters high. A single, short high-amplitude excitation pulse is then applied to the electromagnet, and fast-discharging circuits with special electronic components have even been used to produce such fast pulses.[6] To see the ring jump to 2–3 m high with our setup it would be necessary to reduce the number of turns of the electromagnet coil (say to 100 or even fewer), to use thicker wires, and to apply approximate half-cycle sinusoidal pulses with an order of magnitude more current (say 100 A or more). Reference 6 describes a way to produce large-altitude ring jumps using a capacitor. With larger electrical currents our detection schemes (e.g., the pickup coils) could still be used. The size of the ring is not crucial. Locating the electromagnet core asymmetrically with respect to the coil will reduce the inductance of the electromagnet, thus allowing larger exciting currents. Fortunately, the instantaneous force on the ring could still be determined using our Eqs. (11) and (13), which could then be integrated in closed form (no auxiliary functions such as $b_\rho(z)$ and $b_z(z)$ would then be required). Also note that Figs. 5 and 6 show that it would still be possible for us to follow the upward motion of the ring; in about half a cycle we would be able to register tens of data points.

Our experiments were performed with equipment ordinarily found in a physics laboratory, and we assembled the low-cost setup using either home-made parts or low-cost standard teaching laboratory equipment. Both our theoretical model and our experimental procedures can be extended, for instance, to study the ring flight when a strong pulse of current is applied to the electromagnet. We hope this work will be useful for a senior physics teaching laboratory, to physics teachers at all levels, and to lecturers who demonstrate the Thomson jumping ring.

Two problems that could be posed to a student as an extension are to find a direct method to measure the *motional* emf induced in the ring, and to find the time interval available to transfer momentum to the rising ring. The maximum potential energy $mgh_{\max}$ delivered to the ring is actually equal to the energy absorbed by the motional emf that appears in the ring, and is given by $\int dt\,[vB(2\pi a)]\, i_{\text{ring}}$. Because the length of the core is finite there is a finite time available to transfer momentum to the ring. The maximum height reached by the ring finally becomes constant (saturates) as the number of cycles of applied voltage to the electromagnet increases.

ACKNOWLEDGMENTS

The authors would like to thank the anonymous referees for their valuable comments and recommendations. The authors also warmly thank Professor Gordon Aubrecht for his suggestions and time spent revising the language and style in this paper. Finally, The authors acknowledge the support of Decanato de Investigaciones y Desarrollo of Universidad Simón Bolívar for their support under Grant No. DID-G073.

APPENDIX A: VARIATION OF THE MAIN COIL CURRENT *I* AS A FUNCTION OF THE RING VERTICAL POSITION: THE AUXILIARY FUNCTION *I*(*z*)

To study the z-dependence of the coil current, we use a transformer-like theory of the standard jumping ring setup. The coil of the electromagnet is taken as the primary circuit (resistance R_1 and nominal inductance L_1), while the ring is considered to be the secondary circuit of the transformer (resistance R_2 and nominal inductance L_2). The Variac excites the primary with a voltage V of angular frequency $\omega = 120\pi$ rad/s, and a current i_1 appears in it. If M denotes the mutual inductance between ring and coil, then Kirchhoff's voltage rule for the coil gives

$$j\omega L_1 i_1 + R_1 i_1 = V + j\omega M i_2, \tag{A1}$$

while for the secondary circuit (with no external voltage applied) we have

$$j\omega L_2 i_2 + R_2 i_2 = j\omega M i_1. \tag{A2}$$

Therefore, the current i_2 in the ring is

$$i_2 = \frac{j\omega M}{R_2 + j\omega L_2} i_1. \tag{A3}$$

Substituting this expression into Eq. (A1), we get an equation for the current i_1 in the coil

$$i_1(j\omega L_1 + R_1) = V - \frac{(\omega M)^2}{R_2 + j\omega L_2} i_1, \tag{A4}$$

or

$$\left\{R_1 + \frac{(\omega M)^2 R_2}{{R_2}^2 + \omega^2 {L_2}^2} + j\omega L_1 \times \left[1 - \frac{(\omega M)^2 L_2}{L_1({R_2}^2 + \omega^2 {L_2}^2)}\right]\right\} i_1 = V. \tag{A5}$$

Because $(R_2/\omega L_2)^2 \approx 0.32$ is small,[14] we can neglect the terms in the denominators containing R_2^2 and simplify this equation to

$$\left\{R_1 + \frac{M^2 R_2}{{L_2}^2} + j\omega L_1\left[1 - \frac{M^2}{L_1 L_2}\right]\right\} i_1 = V. \tag{A6}$$

Again, in this equation $M^2 R_2/{L_2}^2 \ll R_1$, and it is also safe to rewrite it as

$$\left\{R_1 + j\omega L_1\left[1 - \frac{M^2}{L_1 L_2}\right]\right\} i_1 = V. \tag{A7}$$

Finally, we can write the main coil current in terms of its own parameters

$$i_1 = \frac{V}{R_1 + j\omega L_1'}, \tag{A8}$$

where L_1' is given by

$$L_1' = L_1\left(1 - \frac{M^2}{L_1 L_2}\right). \tag{A9}$$

As the ring is thrust and travels upward, the coupling mutual inductance M diminishes, whence the coil inductance L_1' increases, and the current in the coil decreases, as can be observed in the upper oscilloscope trace in Fig. 3. In Fig. 11, we have plotted the results of measuring the coil current data, and also plotted the auxiliary function $I(z)$. The mutual inductance M of the ring and the electromagnet coil is a function of z, and a relation to evaluate M will be given in Appendix B.

APPENDIX B: THE emf INDUCED IN THE LONG PICKUP COILS AND THE CURRENT i_{ring} INDUCED IN THE RING

In this Appendix, we derive an additional relation between the emf induced in the long pickup coils and the current i_{ring} induced in the ring (whose mean radius is a) by the excited electromagnet. We begin considering the field created by the ring itself along its z-axis. This is given by a well-known physics textbook relation

$$B_{z,\text{ring}}(z) = \frac{\mu_0\, \mu_r(z)\, i_{\text{ring}} a^2}{2(a^2 + z^2)^{3/2}}, \tag{B1}$$

where μ_0 and $\mu_r(z)$ are the vacuum magnetic permeability and the relative permeability of the electromagnet core, respectively.

Let N and l be the total number of turns and the length of the long pickup coils that surround the core (Fig. 1), respectively. The magnetic flux that appears in the coils is given by

$$\Phi = \int b^2 \frac{\mu_0\, \mu_r(z)\, i_{\text{ring}} a^2}{2(a^2 + z^2)^{3/2}}\, dN, \tag{B2}$$

where b^2 is the core cross sectional area, $dN = (N/l)dz$, and the integral is to be evaluated from $z = -\infty$ to $z = +\infty$. Assuming now that the relative permeability of the core is a slowly varying function of z, i.e., $\mu_r(z) \approx \mu_r$, we get

$$\Phi = b^2 \frac{\mu_0\, \mu_r\, i_{\text{ring}} a^2 N}{2\,l}\left[\frac{z}{a^2(a^2 + z^2)^{1/2}}\right]_{-\infty}^{+\infty} = \frac{b^2 \mu_0\, \mu_r N\, i_{\text{ring}}}{l}. \tag{B3}$$

Finally, the amplitude of the induced emf that appears in the long pickup coils is given by

$$\varepsilon_i = -\frac{d\Phi}{dt} = -\frac{N}{l} b^2 \mu_0 \mu_r \frac{d}{dt} i_{\text{ring}}, \tag{B4}$$

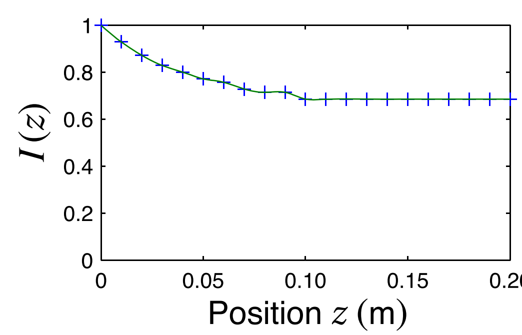

Fig. 11. Auxiliary function $I(z)$ related to the decreasing mutual inductance between the main coil (primary) and ring (secondary). The continuous line is a cubic-spline fitting to the data.

and then the current in the ring can be obtained by integrating the emf that appears in the pickup coils (as explained in Sec. IV above).

Note that the varying mutual inductance between the traveling ring and the electromagnet is given by $M = \phi/i_{\mathrm{ring}}$. This parameter is needed in Appendix A, and can be obtained from Eq. (B2) by changing the limits of the integral in that equation from an initial z (the vertical coordinate of a given ring position) to $(z+l)$, where l is now the length of the main coil. We then obtain the z-dependent mutual inductance

$$M(z) = \pi a^2 \frac{\mu_0 \mu_r N}{2l}\left[\frac{z+l}{\left(a^2+(z+l)^2\right)^{1/2}} - \frac{z}{(a^2+z^2)^{1/2}}\right]. \tag{B5}$$

[a]Electronic mail: clladera@usb.ve

[1]E. J. Churchill and J. D. Noble, "A demonstration of Lenz' law?," Am. J. Phys. **39**, 285–287 (1971).
[2]J. Hall, "Forces on the Jumping Ring," Phys. Teach. **35**, 80–82 (1997).
[3]R. N. Jeffery and F. Amiri, "The phase shift in the jumping ring," Phys. Teach. **46**, 350–357 (2008).
[4]C. S. Schneider and J. P. Ertel, "A classroom jumping ring," Am. J. Phys. **66**, 686–692 (1998).
[5]G. Donoso and C. L. Ladera, "The naked toy model of a jumping ring," Eur. J. Phys. **35**, 015002-1–11 (2014).
[6]F. Washke, A. Strung, and J. P. Meyn, "A safe and effective modification of Thomson's jumping ring experiment," Eur. J. Phys. **33**, 1625–1634 (2012).
[7]In Eq. (3) one would normally write an additional term with the component $dB_{z,m}/dt = (dB_{z,m}/dz)(dz/dt)$. This term corresponds to the motional emf that appears in the ring, and it is less than the term considered in the equation. Note that it takes about 100 ms for the flux to decrease to zero due to the speed of the ring, whereas the ac magnetic flux drops to zero in 1/4 cycle or about 4 ms.
[8]R. P. Feynman, R B. Leighton, and M. Sands, *The Feynman Lectures on Physics* (Addison Wesley, Reading, MA, 1964), vol. II.
[9]C. L. Ladera and G. Donoso, "Oscillations of a spring–magnet system damped by a conductive plate," Eur. J. Phys. **34**, 1187–1197 (2013).
[10]N. Derby and S. Olbert, "Cylindrical magnets and ideal solenoids," Am. J. Phys. **78**, 229–235 (2010).
[11]THM 7025 3-axis Hall Magnetometer, Metrolab Instruments SA CH-1228 Geneva (Switzerland).
[12]R. L. Havill and A. K. Walton, *Elements of Electronics for Physical Scientists* (MacMillan, London, 1975), pp. 254–257.
[13]P. Horowitz and W. Hill, *The Art of Electronics* (Cambridge U. P., Cambridge, 1980), pp. 121–122.
[14]The varying inductance of the ring may be written as $L_2 = l(z)L_0$. Here, $L_0 = 0.110$ μH and $R_2 = 70$ $\mu\Omega$ are measured values, and Fig. 10 shows $l(z) \approx 3$ for the initial portion of the ring flight, therefore $(R_2/\omega L_2)^2 \approx 0.32$.

Balopticon

This combination slide and opaque projector is in the collection of historical physics teaching apparatus at Drury University in Springfield, Missouri. It was made by Bausch & Lomb of Rochester, New York, probably about 1925. It was designed to project 3.25x4 inch glass slides that are fed in through a standard shuttle device. The opaque section on the right-hand side projects pages about six inches square that are held in a door opening in the back, and are illuminated by a bright incandescent lamp inside the housing. (Notes and photograph by Thomas B. Greenslade, Jr., Kenyon College)